Covalent Immobilization of Lysozyme on Stainless Steel. Interface Spectroscopic Characterization and Measurement of Enzymatic Activity

ARTICLE *in* LANGMUIR · JULY 2005

Impact Factor: 4.46 · DOI: 10.1021/la0501278 · Source: PubMed

7 AUTHORS, INCLUDING:

Michel J G Minier
École nationale supérieure de chimie de Paris
21 PUBLICATIONS **696** CITATIONS
SEE PROFILE

Lucica Barbes
14 PUBLICATIONS **93** CITATIONS
SEE PROFILE

Claire-Marie Pradier
Pierre and Marie Curie University - Paris 6
170 PUBLICATIONS **2,819** CITATIONS
SEE PROFILE

Covalent Immobilization of Lysozyme on Stainless Steel. Interface Spectroscopic Characterization and Measurement of Enzymatic Activity

Michel Minier,[†] Michèle Salmain,[†] Nadia Yacoubi,[†] Lucica Barbes,[†] Christophe Méthivier,[‡,§] Sandrine Zanna,[‡] and Claire-Marie Pradier*[,‡,§]

Ecole Nationale Supérieure de Chimie de Paris, Laboratoire de chimie et biochimie des complexes moléculaires, UMR CNRS 7576, 11 rue Pierre et Marie Curie, 75231 Paris Cedex 05, France, and Ecole Nationale Supérieure de Chimie de Paris, Laboratoire de physico-chimie des surfaces UMR CNRS 7045, 11 rue Pierre et Marie Curie, 75231 Paris Cedex 05, France

Received January 17, 2005. In Final Form: April 8, 2005

A new strategy aiming at the protection of metallic surfaces against the growth of biofilms is presented here. This work reports the grafting of primary amines by aminosilanization of oxidized stainless steel followed by chemical coupling of the glycosidase lysozyme from hen egg white using glutaraldehyde as homobifunctional cross-linking agent. Controlled characterization of a stainless steel surface by X-ray photoelectron spectroscopy and Fourier transform infrared reflection−absorption spectroscopy at each step enabled the mode of binding, coverage, and orientation of the grafted molecules to be addressed. As a result, the stainless steel samples covered with a covalently immobilized layer of lysozyme showed some lytic activity on a suspension of bacteria *Micrococcus lysodeikticus*.

Introduction

Bacterial colonization resulting from the contact of solid substrates with moisture, contributes to a large number of bacterial infections in relation for instance with medical devices[1] or the food-processing industry and equipment.[2] Biofilms are also responsible for reduction of heat and mass transfer and/or biocorrosion of materials encountered in a wide range of industrial activities.[3,4]

The sequence of steps leading to the formation of biofilms is now fairly well understood.[5] It is admitted that the first step of biofilm building involves rapid adsorption of biomacromolecules such as proteins and polysaccharides that promotes further bacterial attachment by specific recognition or nonspecific interactions. Attachment of bacteria becomes irreversible by production of extracellular polymer substances that entrap the bacteria within the film.

Traditional surface cleaning procedures to get rid of biofilms on materials in contact with food involve the use of detergents or biocides.[6] Unfortunately, these methods may either be not fully efficient against mature biofilms[7−10] or induce some bacterial resistance in relation with the release of biocides in the environment.[11] Another point that must be taken into account is new regulations that considerably restrict the use of biocides in paints or coatings used to protect metallic surfaces in agricultural or marine environments for instance.

These considerations prompted researchers to provide new strategies to protect metallic surfaces from bacterial adhesion and subsequent biofilm growth. The most successful approaches to date are based on the construction of very thin films of poly(ethylene oxide)/poly(ethylene glycol) onto the metallic surfaces.[12,13] These approaches were particularly efficient to inhibit protein adsorption and promising as regards bacterial adhesion on stainless steel substrates.[14−18] Very recently, self-assembled monolayers of dendritic polyglycerols were shown to effectively prevent protein adsorption on gold.[19]

We have devised another approach to prepare biocompatible surfaces of stainless steel, this being the most

* To whom correspondence should be addressed: tel, + 33 1 44 27 55 33; fax, +33 1 44 27 60 33; e-mail, pradier@ccr.jussieu.fr.

[†] ENSCP, Laboratoire de chimie et biochimie des complexes moléculaires (UMR CNRS 7576).

[‡] ENSCP, Laboratoire de physico-chimie des surfaces (UMR CNRS 7045).

[§] Present address : Université Pierre et Marie Curie, Laboratoire de Réactivité de Surface, UMR CNRS 7609, 4 place Jussieu, 75252 Paris cedex 05, France.

(1) Merritt, K.; Hitchins, V. M.; Brown, S. A. *J. Biomed. Mater. Res.* **2000**, *53*, 131−136.

(2) Sharma, M.; Anand, S. K. *J. Food Sci. Technol.* **2002**, *39*, 573−593.

(3) Cloete, T. E. *Mater. Corros.* **2003**, *57*, 520−526.

(4) Videla, H. A. *Int. Biodeterior. Biodegrad.* **2002**, *49*, 259−270.

(5) Murray, B. S.; Deshaires, C. *J. Colloid Interface Sci.* **2000**, *227*, 32−41.

(6) Parkar, S. G.; Flint, S. H.; Brooks, J. D. *J. Appl. Microbiol.* **2004**, *96*, 110−116.

(7) Flint, S. H.; Van den Elzen, H.; Brooks, J. D.; Bremer, P. J. *Int. Dairy J.* **1999**, *9*, 429−436.

(8) Joseph, B.; Otta, S. K.; Karunasagar, I.; Karunasagar, I. *Int. J. Food Microbiol.* **2001**, *64*, 367−672.

(9) Gibson, H.; Taylor, J. H.; Hall, K. E.; Hollah, J. F. *J. Appl. Microbiol.* **1999**, *87*, 41−48.

(10) Taormina, P. J.; Beuchat, L. R. *J. Appl. Microbiol.* **2002**, *92*, 71−80.

(11) Gilbert, P.; McBain, A. J. *Clin. Microbiol. Rev.* **2003**, *16*, 189−208.

(12) Kingshott, P.; Griesser, H. J. *Curr. Opin. Solid State Mater. Sci.* **1999**, *4*, 403−412.

(13) Ostuni, E.; Yan, L.; Whitesides, G. M. *Colloids Surf., B* **1999**, *15*, 1.

(14) Denes, A. R.; Somers, E. B.; Wong, A. C. L.; Denes, F. *J. Appl. Polym. Sci.* **2001**, *81*, 3425−3438.

(15) Zhang, F.; Kang, E. T.; Neoh, K. G.; Wang, P.; Tan, K. L. *Biomaterials* **2001**, *22*, 1541−1548.

(16) Wei, J.; Bagge Ravn, D.; Gram, L.; Kingshott, P. *Colloids Surf., B* **2003**, *32*, 275−291.

(17) Kingshott, P.; Wei, J.; Bagge Ravn, D.; Gadegaard, N.; Gram, L. *Langmuir* **2003**, *19*, 6912−6921.

(18) Wang, Y.; Somers, E. B.; Manolache, S.; Denes, F. S.; Wong, A. C. L. *J. Food Sci.* **2003**, *68*, 2772−2779.

(19) Siegers, C.; Biesalski, M.; Haag, R. *Chem. Eur. J.* **2004**, *10*, 2831−2838.

10.1021/la0501278 CCC: $30.25
Published on Web 05/18/2005

currently encountered material in food, medicine, or marine environment. This strategy is based on the controlled, covalent immobilization of hydrolytic enzymes that could prevent protein or polysaccharide adsorption or even have a bactericidal effect. As an example, we chose the enzyme lysozyme from hen egg white (HEWL). This readily accessible, low molecular weight enzyme cleaves the polysaccharidic component of cell walls of Gram(+) bacteria (muramidase activity) and, as such, may have an inhibiting effect on bacterial adhesion and proliferation. Indeed some sanitizers already include proteases such as trypsin and glycosidases such as lysozyme. A nonenzymatic antimicrobial activity of HEWL has also been shown[20] that may further enhance the surface antibacterial effect. It was recently shown that treatment by a lysozyme solution of stainless steel coupons covered by a biofilm of *Bacillus flavothermus* removed it and had a protecting effect toward further reattachment of cells.[21] Incorporation of lysozyme into polymeric packaging film structure induced a bactericidal effect against *Lactobacillus plantarum*[22] and *Micrococcus lysodeikticus*.[23]

The key point in enzyme immobilization onto solid substrates such as stainless steel is to devise a strategy that preserves its activity. In this context, direct adsorption of HEWL may induce protein denaturation and subsequent loss of enzymatic activity.[24] Release of enzyme from the surface may also occur in the long term. Conversely, controlled covalent chemisorption of HEWL may lead to a strongly attached enzyme, the challenge being to keep its lytic activity.

Several chemical routes have been described in the literature for the covalent immobilization of proteins onto inorganic materials. The most frequent one relies on aminosilanization of these substrates with γ-(aminopropyl)triethoxysilane (APTES) so as to graft a thin layer of reactive amino groups.[25] In aqueous solution, APTES quickly hydrolyzes to yield the highly reactive silane triol APS that may condense to form polysiloxanes. Silanization of minerals occurs by hydrogen bonding, and metalloxane M−O−Si bonds are formed upon film drying.[26] This step is followed by cross-linking of the proteins using the dialdehyde glutaraldehyde (GA) (Figure 1). In this manner, various kinds of proteins including catalytically active enzymes were immobilized on silicon,[27,28] platinum,[29] titanium oxide,[30−32] gold,[33] and some metallic alloys.[34,35]

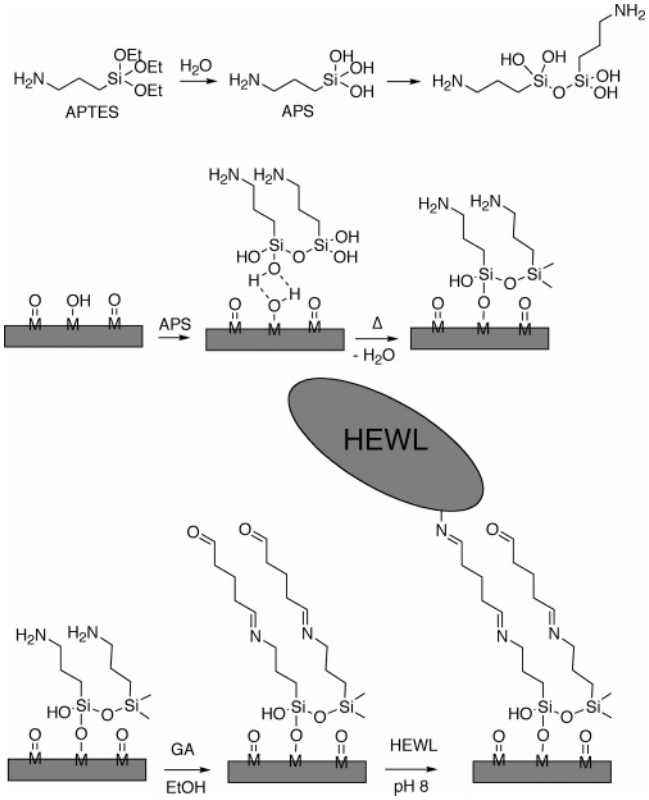

Figure 1. Covalent immobilization of HEWL onto stainless steel.

Interestingly, immobilization of proteins on stainless steel has never been attempted by this route.

We report herein the covalent and controlled immobilization of HEWL to stainless steel AISI 316L coupons previously etched by warm sulfochromic acid treatment. Metallic substrates were characterized after each treatment by X-ray photoelectron spectroscopy (XPS) and Fourier transform infrared reflection−absorption spectroscopy (FT-IRRAS) to get a thorough insight into the atomic and molecular features of the thin organic films. Finally, preliminary enzymatic activity assays were performed on the modified stainless steel coupons and indeed revealed some immobilized lytic activity.

Experimental Section

Materials. γ-(Aminopropyl)triethoxysilane (APTES), glutaraldehyde (GA) 25% in water (w/v), and Bromophenol Blue were obtained from Aldrich and used as received. Hen egg white lysozyme (specific activity 51000 U/mg), crystallized three times, and lyophilized *Micrococcus lysodeikticus* were purchased from Sigma. Sulfuric acid 95% (analytical grade) and potassium bichromate were purchased from Prolabo. AISI 316 L stainless steel coupons ($1.2 \times 1.2 \times 0.1$ cm; area: 3.36 cm^2) were purchased from Goodfellow. They were mechanically polished on one side to 0.25 μm with SiC paper and diamond paste until a mirror finish was obtained. Sulfochromic acid was prepared by dissolution of 6 g of $K_2Cr_2O_7$ per 100 mL of H_2SO_4.

Methods. *Cleaning of Coupons.* After being polished, the coupons were successively ultrasonically washed 5 min in acetone, 5 min in ultrapure water, 15 min in hexane, and 15 min in ultrapure water at 50 °C. This treatment was previously shown to form a stable mixed Cr and Fe oxide and hydroxide passivation layer on top of the substrates.[36] These coupons will be referred to as SS.

(20) During, K.; Porsch, P.; Mahn, A.; Brinkmann, O.; Gieffers, W. *FEBS Lett.* **1999**, *449*, 93−100.
(21) Parkar, S. G.; Flint, S. H.; Brooks, J. D. *J. Ind. Microbiol. Biotechnol.* **2003**, *30*, 553−560.
(22) Padgett, T.; Han, I. Y.; Dawson, P. L. *J. Food Prot.* **1998**, *61*, 1330−1335.
(23) Appendini, P.; Hotchkiss, J. H. *Packag. Technol. Sci.* **1997**, *10*, 271−279.
(24) Lu, J. R.; Su, T. J.; Thirtle, P. N.; Thomas, R. K.; Rennie, A. R.; Cubitt, R. *J. Colloid Interface Sci.* **1998**, *206*, 212−223.
(25) Weetall, H. H. *Appl. Biochem. Biotechnol.* **1993**, *41*, 157−188.
(26) Pape, P. J.; Plueddemann, E. P. *J. Adhes. Sci. Technol.* **1991**, *5*, 831−842.
(27) Wang, Z. H.; Jin, G. *J. Immunol. Methods* **2004**, *285*, 237−243.
(28) Subramanian, A.; Kennel, S. J.; Oden, P. I.; Jacobson, K. B.; Woodward, J.; Doktycz, M. J. *Enzyme Microb. Technol.* **1999**, *24*, 26−34.
(29) Quan, D.; Kim, Y.; Shin, W. *J. Electroanal. Chem.* **2004**, *561*, 181−189.
(30) Jansson, E.; Tengvall, P. *Colloids Surf., B* **2004**, *35*, 45−51.
(31) Jennissen, H. P.; Zumbrink, T.; Chatzinikolaidou, M.; Steppuhn, J. *Materialwiss. Werkstofftech.* **1999**, *30*, 838−845.
(32) Nanci, A.; Wuest, J. D.; Peru, L.; Brunet, P.; Sharma, V.; Zalzal, S.; McKee, M. D. *J. Biomed. Mater. Res.* **1998**, *40*, 324−335.
(33) Raman Suri, C.; Mishra, G. C. *Biosens. Bioelectron.* **1996**, *11*, 1199−1205.
(34) Puleo, D. A. *Biomaterials* **1996**, *17*, 217−222.
(35) Puleo, D. A. *J. Biomed. Mater. Res.* **1997**, *37*, 222−228.
(36) Compère, C.; Bellon-Fontaine, M.-N.; Bertrand, P.; Costa, D.; Marcus, P.; Poleunis, C.; Pradier, C.-M.; Rondot, B.; Walls, M. G. *Biofouling* **2001**, *17*, 129−145.

Table 1. XPS Analysis of Untreated and Treated SS Coupons (Angle = 90°)

	C 1s		O 1s		N 1s		S 2p	
coupon	area	% atomic	area	% atomic	area	% atomic	area	% atomic
SS	18789	29	95459	50.3	1409	1.2	0	0
SS-SC	14308	24.5	96293	56.3	4226	4	5093	5.2
SS-SC-SIL	25214	37.4	87947	44.5	6922	5.7	723	0.6
SS-SC-SIL-GA	29550	41.4	84834	41	7859	5.6	1252	1
SS-SC-SIL-GA-HEWL	38216	53.3	64022	30.5	14354	11.1	0	0

	Si 2p		Cr $2p_{3/2}$		Fe $2p_{3/2}$	
coupon	area	% atomic	area	% atomic	area	% atomic
SS	908	1.7	30465	6.1	75941	10.8
SS-SC	0	0	39388	8.8	3793	0.6
SS-SC-SIL	4020	7.3	21601	4.2	1217	0.2
SS-SC-SIL-GA	4348	7.5	18210	3.3	0	0
SS-SC-SIL-GA-HEWL	2116	3.6	8553	1.6	0	0

Pretreatment of Coupons. SS coupons were further cleaned ultrasonically in acetone for 5 min and then dipped in warm acetone (50 °C) for another 15 min. Coupons were then etched by sulfochromic acid at 60 °C for 10 min and extensively washed with ultrapure water and dried with a flow of N_2. **Caution: Handling of sulfochromic acid should be done in a fume hood, wearing gloves and goggles.** They were kept in a desiccator under vacuum until use (no longer than 2 days[37]). The resulting coupons will be named SS-SC.

Aminosilanization of Coupons. A 0.12% (v/v) solution of APTES in a 3:1 EtOH/H_2O mixture was prepared in a freshly silanized beaker and stirred for 10 min. SS-SC coupons placed in separate silanized glass reactors were covered with 5 mL of this solution for 1−3 min, removed, and dried with a flow of N_2. Coupons were then cured for 1 h at 100−150 °C in air and then washed for 2 min in water to remove physisorbed material.[37] The resulting coupons will be named SS-SC-SIL.

Immobilization of HEWL. SS-SC-SIL coupons were dipped overnight in a solution of GA prepared by mixing 1 volume of the 25% stock solution with 4 volumes of absolute ethanol and then washing with water to yield SS-SC-SIL-GA coupons. **Caution: Handling of GA should be done in a fume hood, wearing gloves and goggles.** They were then dipped overnight in a 1 mg/mL solution of HEWL in 0.1 M phosphate buffer (pH 8.0) at 4 °C and then washed with the same buffer for 15 min and dried with a flow of N_2. For comparison, SS-SC and SS-SC-SIL coupons were directly treated with HEWL in the same conditions and washed similarly.

Surface Analyses. XPS analyses were performed with a VG ESCALAB Mk II spectrometer, using the Al Kα X-ray source (1486.6 eV). A 20 eV pass energy was applied for analyzing the following core level regions: Cr $2p_{3/2}$, Fe $2p_{3/2,5/2}$, O 1s, C 1s, S 2p, Si 2p, and N 1s. The binding energies were calibrated against the binding energy of Au $4f_{7/2}$ and Cu $2p_{3/2}$; with this calibration, the low-energy carbon peak, attributed to hydrocarbon contamination, was measured at 285.4 ± 0.1 eV. The possible error on the peak intensities was estimated to be around 10%. The sensitivity factors of the elements were taken from Scofield;[38] the transmission factor was checked to be constant. In the fitting procedure, no constraint was applied to the initial binding energy values; the full width at half-maximum (fwhm) was set at 1.4 ± 0.2 eV for the carbon contributions, 1.6 ± 0.2 eV for the oxygen contributions, with a Gaussian/Lorentzian ratio (G/L) equal to 80/20.

Fourier transform infrared reflection−absorption spectra (FT-IRRAS) were recorded on a Magna 550 FT-spectrometer (Nicolet) equipped with a Veemax variable angle specular reflectance accessory set at incidence angle of 80°. Six hundred scans were co-added at 8 cm^{-1} resolution and ratioed by the background spectrum of a SS-SC coupon.

Surface Amine Groups Assay. The surface concentration of amine groups was determined by a colorimetric assay using Bromophenol Blue according to a previously published procedure.[39]

Enzymatic Activity Assay. The lytic activity of the stainless steel coupons was measured using the following procedure inspired from the classical lysozyme assay.[40] HEWL-treated coupons placed in separate reactors were covered with 3 mL of a 0.03% (w/v) suspension of *M. lysodeikticus* in 66 mM phosphate buffer, pH 6.24. The reactors were placed on a rocking table, and the suspensions were gently stirred. They were withdrawn every 60 min, and their turbidity was measured spectroscopically at 450 nm (Uvikon 860 spectrometer, Kontron). Two control experiments, whereby the turbidity of a stirred bacterial suspension alone or in the presence of a SS-SC coupon was monitored, were carried out to measure nonenzymatic bacterial lysis (=autolysis). Plots of optical density versus time were generated and slopes measured. By definition, one unit produces a ΔA_{450nm} of −0.001 per min at pH 6.24, 25 °C, using a 0.015% (w/v) suspension of *M. lysodeikticus* in a 2.6 mL reaction mixture.[40] The enzymatic activity of the coupons was calculated using the following equation:

$$\text{enzymatic activity} = [\Delta A_{450nm}(\text{SS-SC-SIL-GA-HEWL}) - \Delta A_{450nm}(\text{SS-SC})]/(-0.001) \times 1.44$$

The correction factor 1.44 results from the product of the volume correction factor, $f_v = 3$ mL/2.6 mL, multiplied by the substrate concentration correction factor, $f_C = 1.25$. This last term comes from the nonlinear dependence of A_{450nm} versus *M. lysodeikticus* concentration and was measured independently.

Results and Discussion

Formation of Silane Film. SS coupons were pretreated with a harsh oxidant, namely, sulfochromic acid, as in a previously described procedure.[37] After the coupons were washed with ultrapure water, the coupons were subjected to XPS analysis.

The substrate peak intensities as well as the elemental chemical composition of the reference (SS) and the etched (SS-SC) metallic surfaces, excluding hydrogen, are reported in Table 1. As reported in a previous publication, the "clean" sample surface layers were constituted of a mixed Cr and Fe hydroxide layer, covered with carbon, and frequently nitrogen, contamination.[41] The hydroxide + oxide layer thickness could be estimated to be close to 30 Å, based on the attenuation lengths calculated from the Seah and Dench formula,[42] and a model developed for the quantitative analysis of passive films on stainless

(37) Chovelon, J. M.; El Aarch, L.; Charbonnier, M.; Romand, M. *J. Adhes.* **1995**, *50*, 43−58.
(38) Scofield, J. H. *J. Electron Spectrosc. Relat. Phenom.* **1976**, *8*, 129−137.
(39) Akkoyun, A.; Bilitewski, U. *Biosens. Bioelectron.* **2002**, *17*, 655−664.
(40) Shugar, D. *Biochim. Biophys. Acta* **1952**, *8*, 302−308.
(41) Pradier, C.-M.; Karman, F.; Telegdi, J.; Kalman, E.; Marcus, P. *J. Phys. Chem. B* **2003**, *107*, 6766−6773.
(42) Seah, M. P.; Dench, W. A. *Surf. Interface Anal.* **1979**, *1*, 2−11.

Table 2. Deconvolution of High-Resolution Cr $2p_{3/2}$ Peak and Measurement of % Areas (Angle = 90°)

	574.4 ± 0.4 eV Cr metal	576.5 ± 0.4 eV Cr=O	578.1 ± 0.4 eV Cr−OH, Cr−O−Si
SS	7.5	69.8	22.6
SS-SC	11.3	71.3	17.5
SS-SC-SIL	7.4	43.9	38.7

Table 3. Deconvolution of High-Resolution O 1s Peak and Measurement of % Areas (Angle = 90°)

	530.4 eV X=O	532.0 eV X−OH	533.2 eV H_2O, Si−O, C−O
SS	58.8	30.1	11.1
SS-SC	32.2	57.3	10.5
SS-SC-SIL	32	39	28.9
SS-SC-SIL-GA	27.6	33.3	39.1
SS-SC-SIL-GA-HEWL	27.4	54.7	27.4

steels by XPS.[43] Most importantly, this contamination layer was shown to be possibly displaced by other molecules upon immersion in proteic solutions for instance. Interestingly, the very aggressive sulfochromic acid treatment induced a strong segregation of Cr to the surface layer at the expense of Fe. The Cr 2p peak could be fitted with three contributions at 574.4 ± 0.4 eV, 576.5 ± 0.4 eV, and 578.2 ± 0.4 eV typical of metallic chromium, chromium oxide, and chromium hydroxide, respectively (see Table 2). Deconvolution of the high-resolution O 1s spectrum confirmed this result; it was indeed fitted with three components at ca. 530.4, 532.0, and 533.2 eV assigned to oxygen in metal oxides, metal hydroxides, or organic oxygen and water, respectively (Table 3). A net increase of the contribution at 532.0 eV was observed for the SS-SC sample, as compared to that of the SS sample. However, it should be noticed on the Cr 2p peak that the hydroxide contribution did not vary significantly. We interpret this apparent discrepancy by a strong hydroxylation of the topmost layer and/or the possible contribution of oxygen in sulfates after the sulfochromic treatment.[44] The latter point seems to be comforted by the net increase of the sulfur peak intensity. Note eventually that deposition of Cr oxide from sulfochromic treatment may also explain the increase of the Cr surface fraction. This surface hydroxylation should in principle favor the subsequent chemisorption of APTES as the generally admitted mechanism of silanization of inorganic materials first involves the formation of hydrogen bonds between silanols (resulting from the hydrolysis of the Si−OR bonds) and hydroxides (Figure 1).

A high level of carbon was also detected on the SS-SC coupon (see Figure 2). The C 1s spectrum was best fitted with three contributions at 285.1 (main contribution), 286.7, and 288.7 eV assigned to C−C plus C−H, C−O, and C=O, respectively (Table 4). The presence of hydrocarbons and carbonates from adventitious contamination and possibly remaining ethanol after rinsing procedures may explain these peaks. Finally, a low amount of contaminating N was also detected for the SS-SC coupon; it appears to be higher than before etching procedure likely because of a decrease of the carbon contamination.

SS-SC coupons were treated with a hydro-alcoholic solution of APTES, applying a previously optimized procedure.[37] Samples cured at high temperature were submitted to XPS analysis. Binding of APTES was assessed by the decrease of the Cr and Fe substrate signals and by the concomitant increase of the C 1s, N 1s, and Si 2p peaks. However, the metal atoms were still detectable, indicating that the organic film was thin. The average thickness, calculated from the attenuation of chromium, was found to be equal to 11 Å, a value slightly larger than the calculated length of 8 Å for a fully extended APS molecule suggesting that, on an average, a monolayer film of APS has been formed. For this calculation, the formula, $I/I^\circ = \exp(-d/\lambda \sin \theta)$ was used, where I/I° is the Cr 2p intensity ratio, d is the film thickness, θ the angle between the analyzer and the surface parallel (takeoff angle), and λ the attenuation length of Cr 2p photoelectrons through an organic layer. λ was taken equal to 29 Å, using the formula established by Whitesides et al.[45] for ordered thiol SAMs.

The Cr 2p peak was fitted with metal, oxide, and hydroxide contributions with a relative increase of the last one; this is likely to be due to the formation of metalloxane M−O−Si bonds (M = Cr or Fe). The oxygen peak intensity slightly decreased too, due to the attenuation of the oxide surface by the polysiloxane film that overcomes the gain of oxygen from siloxane molecules. Three components were again visible on the O 1s peak (see Figure 3), with a net increase of the contribution at 533.2 eV at the expense of the 532.0 eV hydroxide contribution (Table 3). This confirms the presence of new Si−O bonds. The C 1s peak was again fitted with three contributions (Figure 2) with a net increase of the one at 286.7 eV; this is clearly due to carbon in Si−C or N−C bonds coming from the newly attached compound. Let us notice that the position of the Si $2p_{3/2}$ peak at 102.9 eV is typical of silicones.[46] Finally, the high resolution N 1s spectrum (Figure 3) was fitted with two components at 400 and 401.6 eV (Table 5). These contributions were assigned to unprotonated and protonated N atoms, respectively.[46]

The binding mode of APTES to iron and chromium oxides[47] and to different kinds of steel[48−51] has been previously studied, and the reported results are somewhat contradictory as regards the metal−organosilane interface. Time-of-flight secondary ion mass spectrometry (ToF-SIMS) analysis of APS film on cold-rolled steel deposited from an aqueous solution at pH 10.4 indicated that the film was very thin and the orientation of the APS molecules was in part with the silanol groups and in part with the amino groups adsorbed at the film−steel interface, the nitrogen atoms being protonated in the latter case.[48] Most importantly, no metalloxane bonds were detected in the conditions to form the film. Other ToF-SIMS experiments completed by XPS analyses showed that the orientation of the molecules depended on the time of contact of the metallic substrates with the APS solution.[50] XPS studies of APS films on iron and chromium oxides had also shown that the surface nitrogen atoms were partially protonated. This finding was related either to intramolecular hydrogen bonding between the silanols and the basic amines (Figure 4B) or to the interaction of the amino groups with surface hydroxyl groups (Figure 4C) with a preference for the

(43) Vito, E. D.; Marcus, P. *Surf. Interface Anal.* **1992**, *19*, 403−408.
(44) Stypula, B.; Stoch, J. *Corros. Sci.* **1994**, *36*, 2159−2167.
(45) Laibinis, P. E.; Chain, C. B.; Whitesides, G. M. *J. Phys. Chem.* **1991**, *95*, 7017−7021.
(46) Wagner, C. D.; Riggs, W. M.; Davies, L. E.; Moulder, J. F. *Handbook of X-ray photoelectron* spectroscopy, 1st ed.; Perkin-Elmer Corp. (Physical Electronics Division): Eden Prairie, MN, 1979.
(47) Horner, M. R.; Boerio, F. J.; Clearfield, H. M. *J. Adhes. Sci. Technol.* **1992**, *6*, 1−22.
(48) van Ooij, W. J.; Sabata, A. *J. Adhes. Sci. Technol.* **1991**, *5*, 843−863.
(49) Puomi, P.; Fagerholm, H. M. *J. Adhes. Sci. Technol.* **2001**, *15*, 869−888.
(50) Quinton, J. S.; Dastoor, P. C. *Surf. Interface Anal.* **2000**, *30*, 21−24.
(51) Harun, M. K.; Lyon, S. B.; Marsh, J. *Prog. Org. Coatings* **2003**, *46*, 21−27.

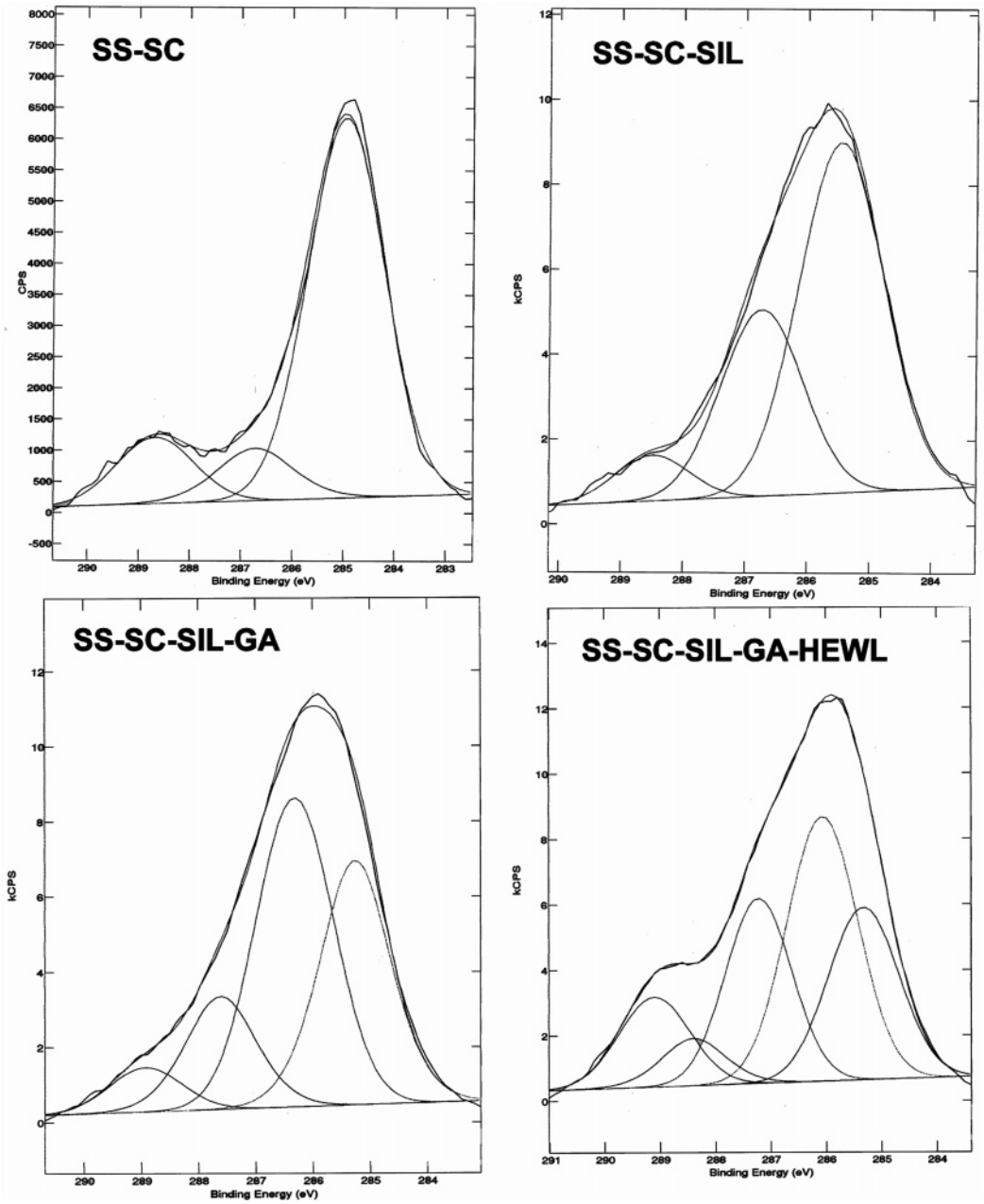

Figure 2. High-resolution C 1s spectra of stainless after successive chemical treatments.

Table 4. Deconvolution of High-Resolution C 1s Peak and Measurement of % Areas (Angle = 90°)

	C 1s A		C 1s B		C 1s C		C 1s D		C 1s E	
coupon	BE, eV	%	BE, eV	%	BE, eV	%	BE, eV	%	BE, eV	%
SS-SC	285.1	76.2	286.7	11			288.7	12.9		
SS-SC-SIL	285.3	60.7	286.7	32.5			288.5	6.8		
SS-SC-SIL-GA	285.3	32.4	286.3	46.1	287.3	15.7	288.6	5.8		
SS-SC-SIL-GA-HEWL	285.3	22	286.3	36.4	287.2	23.8	288.4	6	289.1	11.8

second explanation. The orientation of APS molecules depicted in Figure 4C was confirmed by a more recent XPS study of APS films on mild steel.[51] However, these results referred to uncured substrates. Curing of metallic substrates was reported to stabilize APS films on hot-dip galvanized steel.[49] This stabilization may be attributed to the formation of M−O−Si and Si−O−Si bonds resulting from film dehydration to yield a two-dimensional polymeric network.[25,28]

We ran an angle-resolved XPS analysis of the APS film to try and gain an insight into the orientation of the APS molecules within the organic film among all the possible configurations depicted in Figure 4. At a 90° takeoff angle, the N/Si ratio was equal to 0.78 ± 0.08. This value, which is below the theoretical ratio of unity, seems to indicate that Si atoms are, on an average, above the N atoms (Table 6). This ratio decreased to 0.65 ± 0.08 at a 45° takeoff angle, confirming that the APS molecules were partially oriented with the nitrogen atoms in direct contact with the metal surface. Nonetheless let us recall that the proportion of protonated nitrogen atoms is 30% (see Table 5); hence some of the surface amino groups should be available for further reactions. Indeed an independent colorimetric assay of surface amine groups performed on

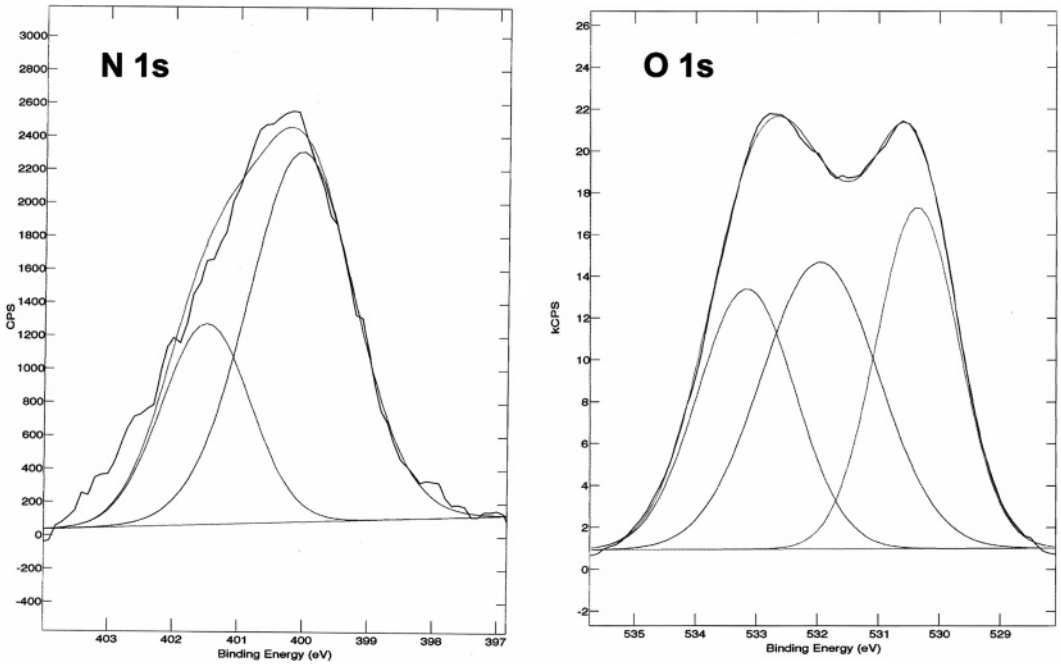

Figure 3. High-resolution N 1s and O 1s spectra of SS-SC-SIL coupon.

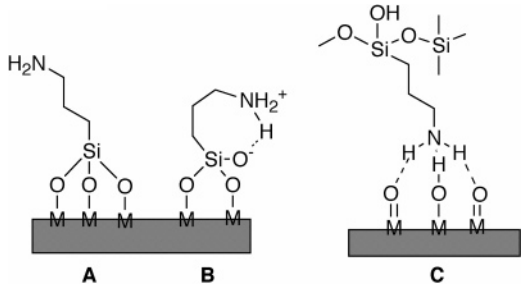

Figure 4. Possible schematic modes of binding of APS to stainless steel surface.

Table 5. Deconvolution of High-Resolution N 1s Peak and Measurement of % Areas (Angle = 90°)

	400.0 eV NH_2	401.6 eV NH_3^+
SS-SC-SIL	70	30
SS-SC-SIL-GA	75	25
SS-SC-SIL-GA-HEWL	90	10

Table 6. Comparison of N/Si Atomic Ratios at 90 and 45° Angle Analysis

coupon	N/Si (90°)	N/Si (45°)
SS-SC-SIL	0.78	0.65
SS-SC-SIL-GA	0.82	nd
SS-SC-SIL-GA-HEWL	3.08	nd

SS-SC-SIL samples gave a value of 0.57 ± 0.16 $NH_2/100$ Å^2 ($n = 8$). By comparison, the calculated surface amine concentration of a monolayer of APS on silica was shown to range from 1 to 3 $NH_2/100$ Å^2.[52] We may then infer that the APS molecules within the organic film adopt all the conformations illustrated in Figure 4, including orientation of the N atoms toward the metal oxide/hydroxide surface.

The APS film was further analyzed by FT-IRRAS. To facilitate band assignments, the IR spectrum of bulk APTES was recorded and compared to the IRRAS spectrum of the APS film (Figure 5). Assignments were done based on handbook values (Table 7).[53]

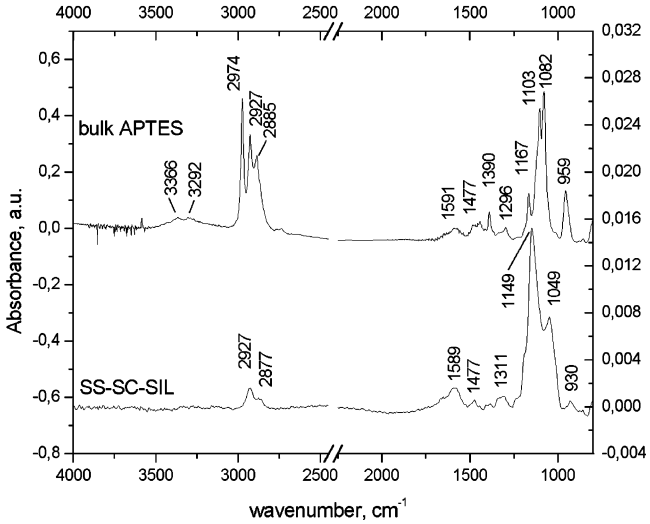

Figure 5. IR (thin film) spectrum of APTES and IRRAS spectrum of SS-SC-SIL coupon.

Table 7. Comparison of IR Spectra of Bulk APTES and APS Film of Stainless Steel

bulk APTES, cm^{-1}	intensity	APS film, cm^{-1}	assignment
3366	w		ν(N−H) as
3292	w		ν(N−H) s
2974	s		ν(C−H) as (CH_3)
2927	s	2927	ν(C−H) as (CH_2)
2885	s	2877	ν(C−H) s (CH_2)
1591	w	1589	δN−H
1477	w	1477	δ(CH_2) scissoring vibration
1390	m		δ(C−H) (CH_3)
1296	w	1311	CH_2 wagging
1167	s		ν(C−O) as (EtO)
1103	vs	1149	ν(Si−O−C) as or ν(Si−O-M)
1082	vs	1049	ν(Si−O−C) as or ν(Si−O−Si)
956	s		ν(Si−O−C) s
	w	930	ν(Si−OH)

Very noticeable differences between the IR spectrum of pure APTES and APS film were observed. First, all the

(52) Puleo, D. A. *J. Biomed. Mater. Res.* **1995**, *29*, 951−957.

(53) Socrates, G. *Infrared characteristic group frequencies*; Wiley-Interscience: Chichester, 1980.

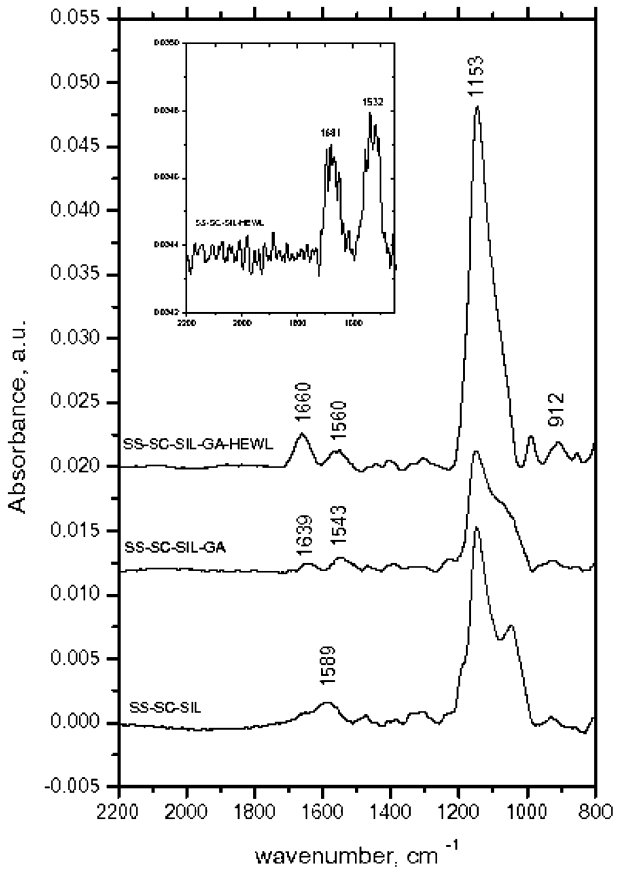

Figure 6. IRRAS spectra of SS-SC-SIL, SS-SC-SIL-GA, and SS-SC-SIL-GA-HEWL. Inset: IRRAS spectrum of SS-SC-SIL-HEWL.

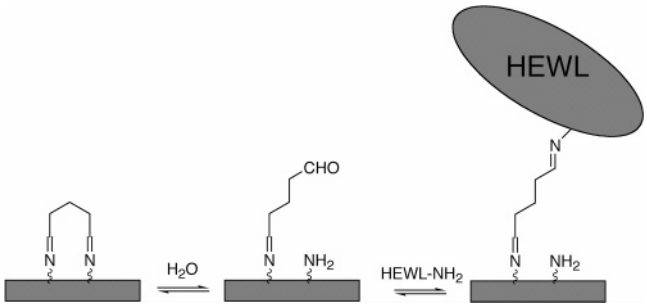

Figure 7. Chemical coupling of HEWL to GA layer.

vibrations corresponding to the ethoxy groups ($\nu(CH_3)$, $\delta(CH_3)$, $\nu(C-O)$, and $\nu(Si-O-C)$) are missing from the APS film IR spectrum, indicating that APTES was fully hydrolyzed when adsorbed onto the SS-SC surface. This is in complete agreement with previously reported results.[49,54] Moreover, APTES has been shown to hydrolyze during the time the solution was aged.[37] Second, the frequency of the two asymmetric stretching vibrations of Si−O bonds was shifted. This change may be assigned to the formation of Si−O−M (M = Cr or Fe) and Si−O−Si bonds in agreement with the expected mechanism of condensation of silanes to metal oxides/hydroxides. A very weak band at 930 cm^{-1} that we assigned according to previously published data to the stretching Si−OH vibration[54] indicates that silanols are also present in the film.

On the whole and combining XPS and FT-IRRAS data, it clearly appears that an organosilane film was formed by contact of sulfochromic acid-etched SS samples with an aqueous solution of APTES followed by curing at high temperature. The film structure and the mode of binding of APS to SS appeared to be in agreement with previously published data, i.e., hydrolysis of Si−OEt bonds of APTES to generate Si−OH that further partially condenses into polysiloxanes and metalloxanes. Binding of APS by hydrogen bonding of the primary amine to surface oxides/hydroxides was also shown to occur as evidenced by XPS data.

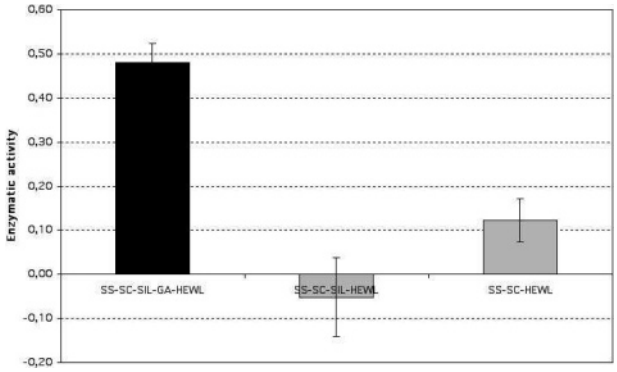

Figure 8. Enzymatic activity of several lysozyme-treated stainless steel coupons on *Micrococcus lysodeikticus* suspension. See experimental conditions in text.

Immobilization of HEWL. To covalently attach HEWL to the amine-containing silane layer, a cross-linker is needed. The dialdehyde glutaraldehyde provides a convenient means to cross-link proteins via their free amino groups (lysines and the N-terminal group) to aminated solid substrates.[25] It readily condenses with primary amines to yield Schiff bases, providing a convenient way to conjugate two amine-containing molecules together. The five-carbon-atom chain length of the cross-linker may also enable an increase in the distance between the protein and the metallic surface. SS-SC-SIL coupons were treated by an ethanolic solution of GA, and surface analysis was again done by XPS and FT-IRRAS. The XPS spectra revealed again an attenuation of the Cr and Fe signals and an increase of the C 1s peak intensity (Table 1). The latter finding was explained by the addition of five carbons brought by the binding of GA while the former indicated that the organic layer thickness increased. It was now equal to 18 Å; note that the average thickness is very close to the one expected for a monolayer of fully extended glutaraldehyde molecules calculated to be 17 Å. The percentage of the other elements and the N/Si atomic ratio remained unchanged (Table 5).

On the high-resolution C 1s spectrum of the SS-SC-SIL-GA coupon, a new component at 287.3 eV was now observed (Figure 2) and assigned to the C of the C=N and/or C=O bonds of the GA molecules. A weak contribution at 288.6 eV, likely due to carbonates, was still visible. Again, the total oxygen intensity did not vary but a significant increase of the 533.2 eV component was noticed (Table 3), corresponding to an increase in the organic oxygen amount, probably oxygen from water molecules left after rinsing the sample. The O 1s low BE contribution slightly decreased, despite the new aldehyde functions. We ascribe this to the stronger attenuation of the oxide layers.

A slight change of the IRRAS spectrum of the SS-SC-SIL-GA coupon was also observed (Figure 6). The weak $\delta(N-H)$ band disappeared while two weak new bands were now observed at 1639 and 1543 cm^{-1}. The former one may be assigned to the C=N stretching vibration while the

(54) Subramanian, V.; van Ooij, W. J. *Corrosion* **1998**, *54*, 204−215.

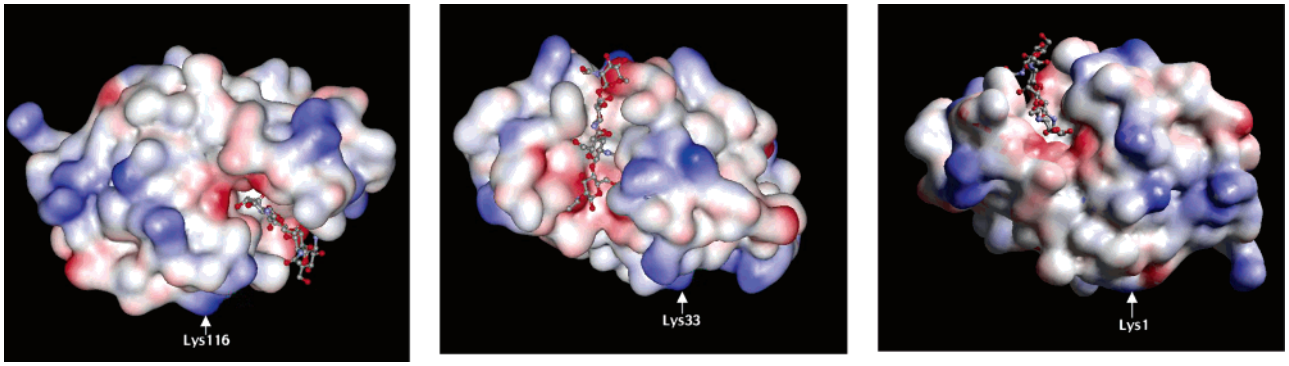

Figure 9. Molecular models of HEWL−NAG_4 complex drawn from the X-ray structure (PDB file 1LZC) pointing out three of the six lysines of HEWL. Drawings generated with WebLab ViewerLite.

latter might correspond to the symmetric $\delta(NH_3^+)$. Interestingly, the C═O stretching vibration of the aldehyde group expected at ca. 1730 ± 10 cm^{-1} was absent from the spectrum. Two reasons might be put forward to explain this finding. First, the C═O bonds might be oriented parallel to the metal surface and therefore not detectable by IRRAS, as this surface analytical technique is sensitive to vibrator orientation. Second, no free aldehyde groups may be present in the organic film. Considering the flexible structure of GA, two neighboring amines may have reacted to form a cyclic diimine. This structure may however still be reactive toward other amines as the Schiff base condensation is known to be a reversible process (Figure 7).[55]

A SS-SC-SIL-GA coupon was treated with a buffered solution of lysozyme at slightly basic pH, as this condition should favor condensation between the surface aldehydes and the protein amines. The resulting SS-SC-SIL-GA-HEWL coupon was analyzed by XPS (Table 1). The C and N fractions were seen to significantly increase while the apparent amount of O, Si, Cr, and Fe decreased due to the stronger substrate attenuation. Let us note, however, that the metal signals were still detected. The C 1s high-resolution spectrum was again changed with a marked increase of the high BE contributions, now including a new component at 289.1 eV, corresponding to C(═O)O and C(═O)NH groups (Table 4 and Figure 2).[56] Deconvolution of the high-resolution N 1s spectrum showed that most of the N atoms were now in the deprotonated form (peptide bonds) (Table 5). This body of results gave good evidence for the presence of protein molecules on the surface. The total average thickness layer was now equal to 23 Å, i.e., an increase of 5 Å. As a point of comparison, the molecule of lysozyme can roughly be assigned to an ovoid of 32 Å by 45 Å, as measured on the published high-resolution X-ray structure.[57] The atomic N/Si ratio was now equal to 3.08 (Table 6). The theoretical N/Si ratio can be calculated as follows. A molecule of lysozyme theoretically occupies an area of 32 Å × 45 Å = 1440 $Å^2$ whereas a molecule of APS occupies an area of 50 $Å^2$ in a monolayer (see above). One molecule of lysozyme covers 1440/50 = 29 molecules of silane. Each molecule of lysozyme includes 176 N atoms. The theoretical N/Si for a full monolayer of lysozyme on a monolayer of APS is then 1 + 176/29 = 7.7 not taking into account the attenuation of the Si signal by the organic overlayer. It appears, from the comparison between the theoretical and the actual N/Si ratios, that surface coverage is below 40%.

The 1500−1700 cm^{-1} spectral region of the IRRAS spectrum of the SS-SC-SIL-GA-HEWL coupon displayed two typical bands at 1660 and 1560 cm^{-1}, readily assigned to the amide I and amide II vibrations of the polypeptide backbone of HEWL (Figure 6).

Thus, both XPS and IRRAS bring complementary evidence that the enzyme HEWL was bound to the stainless steel surface, but its surface coverage was probably less than one monolayer.

Enzymatic Activity Assay. Lysozyme is a glycosidase that cleaves the polysaccharidic component of the cell wall of bacteria such as *M. lysodeikticus*, inducing cell lysis. To evaluate its enzymatic activity, coupon SS-SC-SIL-GA-HEWL was immersed in a suspension of *M. lysodeikticus* and its turbidity was monitored spectrophotometrically during 6 h. Other experiments were performed to assess the efficiency of the immobilization procedure. SS-SC and SS-SC-SIL coupons were dipped overnight in a solution of HEWL. The enzymatic activity of the resulting SS-SC-HEWL and SS-SC-SIL-HEWL samples was assayed on the *M. lysodeikticus* suspension accordingly. To correct from nonspecific effects, the turbidity of a bacteria suspension alone or in the presence of a bare SS-SC coupon was monitored in parallel.

The enzymatic activity calculated for the various samples (see Experimental Section) is reported in Figure 8. An enzymatic activity of 0.5 U was measured for sample SS-SC-SIL-GA-HEWL. The specific activity of lysozyme in solution was 51000 U/mg; thus the immobilized activity was equivalent to ca. 10 ng of enzyme in solution. On the other hand, a full monolayer of lysozyme corresponds to 3.36×10^{16} $Å^2/1440$ $Å^2 = 2.33 \times 10^{14}$ molecules, i.e., 550 ng of protein (MW = 14300). In the previous section, we estimated the maximum surface coverage of lysozyme to be 40% of a full monolayer, i.e., 550 × 0.4 = 220 ng. The large difference between the equivalent quantity of immobilized enzyme and this maximum surface coverage estimation reflects that the enzymatic activity of immobilized lysozyme is probably lower than that of the enzyme in solution. To explain the partial loss of enzymatic activity of lysozyme upon immobilization, it should be recalled that although none of the six lysines of lysozyme is included in the catalytic site,[58,59] covalent binding to the stainless steel samples via some of these residues may result in orientations where the enzyme active site is not accessible to the substrate because of steric hindrance. Different views of the molecular model of the lysozyme−NAG_4 complex (pdb file 1LZC; NAG_4 is tetra-*N*-acetyl-

(55) Means, G. E.; Feeney, R. E. *Anal. Biochem.* **1995**, *224*, 1−16.
(56) Boonaert, C. J. P.; Dufrëne, Y. F.; Derclaye, S. R.; Rouxhet, P. G. *Colloids Surf., A* **2001**, *22*, 171−185.
(57) Broutin, I.; Riès-Kautt, M.; Ducruix, A. F. *J. Cryst. Growth* **1997**, *181*, 97−108.
(58) Smith, L. J.; Sutcliffe, M. J.; Redfield, C.; Dobson, C. M. *J. Mol. Biol.* **1993**, *229*, 930−944.
(59) Blake, C. C. F.; Koenig, D. F.; Mair, G. A.; North, A. C. T.; Phillips, D. C.; Sarma, V. R. *Nature* **1965**, *206*, 757−761.

chitotetraose)[60] depicted in Figure 9 show that enzyme bound via lysine 116 is highly unfavorable as regards enzymatic activity whereas enzymes bound via lysines 1 or 33 are more favorable.

Conversely, no significant enzymatic activity was observed for coupons SS-SC-HEWL and SS-SC-SIL-HEWL. This latter result may just be observed because HEWL was not able to bind to SS coupons in the experimental conditions. To check this hypothesis, we proceeded to the IRRAS analysis of the SS-SC-HEWL and SS-SC-SIL-HEWL coupons (Figure 6, inset). The two typical amide I and amide II bands were observed on the spectra, indicating that HEWL indeed adsorbed to both substrates. However, the position of these bands was pretty much different from that recorded for the SS-SC-SIL-GA-HEWL coupon with the amide I band at 1681 and the amide II band at 1532 cm^{-1}. This may indicate that the secondary and/or tertiary structures of HEWL were greatly altered when directly adsorbed to the SS coupon even when it was covered with the APS film. This alteration of the structure of the enzyme might have in turn led to the loss of its catalytic activity.

Conclusions

This work reports on the immobilization of a hydrolytic enzyme, namely, lysozyme, to the surface of stainless steel as a new way to protect the surface against the growth of biofilms. The stainless steel surface was activated, silanized with APTES, and functionalized with glutaraldehyde to ensure a covalent binding of the protein. FT-IRRAS and XPS, run at each step of the surface modification, demonstrated that silanization and chemical linkage of glutaraldehyde did occur, leading to quasi-complete molecular layers. Binding of the enzyme was indeed achieved, but coverage was low partly due to a misoriented binding of APTES. Nonetheless, the weak amounts of lysozyme molecules that were immobilized on the stainless steel surface provided a significant lytic activity. Forthcoming studies should now address the immobilization of a larger amount of catalytically active enzyme molecules, either by better controlling the silanization step or by using another linking molecule, for instance a polymer. The final step will of course be cell adhesion tests on the enzyme-modified surfaces.

Acknowledgment. This work was financially supported by The Centre National de la Recherche Scientifique, the French Ministry of Research, and the FP5 European program "Marie Curie Training Site" (Contract No. HMPT-CT-2000-00186).

LA0501278

(60) Maenaka, K.; Matsushima, M.; Song, H.; Sunada, F.; Watanabe, K.; Kumagai, I. *J. Mol. Biol.* **1995**, *247*, 281−293.